A Strategy to Find Minimal Energy Nanocluster Structures

José Rogan,[a] Alejandro Varas,[a,b] Juan Alejandro Valdivia,[a] and Miguel Kiwi*[a]

An unbiased strategy to search for the global and local minimal energy structures of free standing nanoclusters is presented. Our objectives are twofold: to find a diverse set of low lying local minima, as well as the global minimum. To do so, we use massively the fast inertial relaxation engine algorithm as an efficient local minimizer. This procedure turns out to be quite efficient to reach the global minimum, and also most of the local minima. We test the method with the Lennard–Jones (LJ) potential, for which an abundant literature does exist, and obtain novel results, which include a new local minimum for LJ_{13}, 10 new local minima for LJ_{14}, and thousands of new local minima for $15 \leq N \leq 65$. Insights on how to choose the initial configurations, analyzing the effectiveness of the method in reaching low-energy structures, including the global minimum, are developed as a function of the number of atoms of the cluster. Also, a novel characterization of the potential energy surface, analyzing properties of the local minima basins, is provided. The procedure constitutes a promising tool to generate a diverse set of cluster conformations, both two- and three-dimensional, that can be used as an input for refinement by means of *ab initio* methods. © 2013 Wiley Periodicals, Inc.

DOI: 10.1002/jcc.23419

Introduction

The first and crucial step in the description and understanding of nanostructures, like clusters, is the precise determination of the geometrical structure that their constituent atoms do adopt. This was lucidly formulated by Goedecker et al.[1]: "Determining the structure of a molecule, cluster, or crystal is one of the most fundamental and important tasks in solid state physics and chemistry. Practically, all physical properties depend on its structure." During the last years, a variety of techniques such as Monte Carlo,[2,3] Big-Bang,[4] genetic algorithm (GA),[5–7] conformational space annealing,[8–10] Basin Hopping (BH),[11] among others, have been used to determine minimum energy cluster configurations, with varying degree of success. Many variations and alternative procedures have been put forward, like the one by Goedecker[12] who focuses on obtaining the global minimum by means of an interesting and ingenious method, which reduces repeated visits to the same attraction basin by "flooding" it. Goedecker also coupled his methodology with electronic structure codes.

Our objective is twofold: to develop a method which allows to obtain a large amount (presumably a majority) of the local minima, and which also has the capability of efficiently finding the global minimum. Most procedures focus their interest on the global minimum, while we try to generate a set of minima which includes both the global minimum, and a large diversity of local minima. In this context, we develop a simple strategy, based on the fast inertial relaxation engine (FIRE) minimizer, to satisfy both objectives. FIRE is a novel and efficient algorithm put forward by Bitzek et al.,[13] who describe it as a method based on conventional molecular dynamics, with additional velocity modifications and adaptive time steps. FIRE is a simple local atomic structure optimization algorithm, which is quite efficient and has been widely used in several closely related contexts, and by various authors. Most recently by Machado,[14] the Goedecker group,[15,16] and by Ishii et al.,[17] who in addition provide a critical discussion on the procedure and extensive references. However, while our implementation has much in common with the work just mentioned, and with older papers that can be found in the literature, it also has significant differences which will be detailed below.

We focus our interest on the Lennard–Jones (LJ) potential, for which there is a wide literature and many well-established results. However, the procedure is by no means restricted to LJ-type interactions between atoms. In fact, it seems to be transferable, and to this effect we will also provide results obtained, by means of our strategy, for another well-established potential: the one due to Morse.[18,19] Moreover, the procedure is not restricted to classical potentials, to which we limit ourselves for the time being, but we have obtained some preliminary results for small clusters using it in combination with *ab initio* calculations.

This article is organized as follows: in section Methodology, we describe the computational methods implemented in our study. In section Results, we report on specific issues such as the global minima, number of local minima, volumetric and planar minima, minima distributions, and the size of the

[a] *J. Rogan, A. Varas, J. A. Valdivia, M. Kiwi*
Departamento de Física, Facultad de Ciencias, Universidad de Chile, Casilla 653, Santiago, Chile 7800024, and Centro para el Desarrollo de la Nanociencia y la Nanotecnología (CEDENNA), Avda., Ecuador 3493, Santiago, Chile 9170124
E-mail: m.kiwi.t@gmail.com

[b] *A. Varas*
Departamento de Física de Materiales, Nano-Bio Spectroscopy Group and ETSF Scientific Development Centre, Universidad del País Vasco UPV/EHU, Av. Tolosa 72, E-20018 San Sebastián, Spain

Contract grant sponsor: Fondo Nacional de Investigaciones Científicas y Tecnológicas (FONDECYT, Chile); Contract grant numbers: 1090225, 1120399, and 1130272 (J.R. and M.K.) and 1110135 (J.A.V.); Contract grant sponsor: Financiamiento Basal para Centros Científicos y Tecnológicos de Excelencia

attraction basins. And finally, in section Discussion and Conclusion, we draw conclusions and close this article.

Methodology

The purpose of the strategy we develop here is to obtain a set of local minima, as complete as possible, which is expected to include the global minimum. We use the words "global minimum" as the established one, but do not exclude the possibility that a lower one can eventually be found. The procedure also allows to determine how often a particular local minimum is reached, which yields information on the relative basin size of that minimum of the potential energy surface (PES). Even though it is not possible to be certain that all the minima of a PES have been found, the use of a variant of the rarefaction plot[20–23] provides an estimate on how many seeds should be minimized to obtain, if not all, at least most of the minima for a particular PES. The rarefaction curve is a resource taken from ecology, and basically is a graph of the number of hits (different local minima) as a function of the number of seeds that are examined, which in addition is useful to characterize diversity, and on which we will elaborate later on.

The FIRE method

We have chosen to use the FIRE algorithm to obtain the minimal energy structures, instead of conjugate gradient or L-BFGS,[24] because it is strictly local, it does not get stuck in transition states, and is a very efficient procedure. The FIRE algorithm is described by Bitzek et al.[13] as a fast optimization method, based on conventional molecular dynamics, with additional velocity modifications and adaptive time steps Δt. However, the experience we developed performing the calculations taught us that special care has to be given to the initial Δt value, because it strongly influences the number of force evaluations that are required, and therefore the overall computing speed of the procedure. The major difficulty one faces with a method, as the one just mentioned, is the determination of the number of seed configurations that are necessary to be "reasonably" sure that one does obtain an overwhelming majority of all the minima.

In the context of diversity, our strategy considers two configurations as the same if their energies differ by less than a critical value. It is worth mentioning that one might expect to find two structures that have the same energy, but are geometrically different. However, we verified that for $N \leq 16$ this does not occur. To test this assertion, we also filtered the full-configuration set using the similarity criterion put forward by Grigoryan and Springborg,[25] which can be defined as follows: two N atom clusters, A and B, are similar if

$$D_{A,B} = \left[\frac{2}{N(N-1)} \sum_{i=1}^{N(N-1)/2} \left(d_i^{(A)} - d_i^{(B)} \right)^2 \right]^{1/2} < D_c \,. \qquad (1)$$

Here, $d_i^{(A)}$ is the sorted list of $N(N-1)/2$ interatomic pair distances of cluster A (and similarly for B), and D_c is a critical value. This measure has the significant advantage of being translationally and rotationally invariant, and furthermore it is fast and simple to evaluate. In all the calculations, we also computed the energy ordering, and we verified that both the similarity criterion of eq. (1), and the energy ordering, yield identical sets of diverse configurations for $N \leq 16$. However, due to the enormous amount of local minima that are found for large N clusters, we cannot establish if this property is general or limited to rather small N values.

The problem of the precise characterization of the structural diversity has yet to find a complete solution. However, it is not the purpose of this article to settle this issue. The distance we use, as given by eq. (1), works adequately for the small clusters we deal with here, but a lucid discussion of this matter, and the many intricacies it has for larger clusters, can be found in a publication by Oganov and Valle.[26]

The LJ potential

We now illustrate our strategy, and apply it to the problem of an N-atom clusters. The main interaction potential we adopt is the LJ pair potential, which for several decades has been used as a benchmark for cluster energy minimization methods, and which even today constitutes a challenging and active area of research.[27–29]

The LJ pair potential can be defined as follows:

$$E_{\mathrm{LJ}_N} = 4\varepsilon \sum_{i=1}^{N-1} \sum_{j=i+1}^{N} \left[\left(\frac{\sigma}{r_{ij}} \right)^{12} - \left(\frac{\sigma}{r_{ij}} \right)^{6} \right], \qquad (2)$$

where N is number of atoms in the cluster, r_{ij} is the distance between atoms i and j, ε is the potential well depth, and σ determines the equilibrium pair separation. The LJ potential has been extensively investigated in the context of cluster configurations. The LJ global minima, and the number of local minima up to $N = 14$, can be found in the Cambridge Cluster Database.[30] In spite of these efforts, our strategy has shown its power by allowing us to find several unreported minima: one new local minimum for LJ_{13}, 10 new local minima for LJ_{14}, and thousands of local minima for LJ_N, with $15 \leq N \leq 65$.

Our procedure, to obtain the energy minima for an N atom cluster, and which is somewhat different from other FIRE applications, is setup by generating at random a set of $3N$ coordinates, in a cubic box of volume a^3, which we denominate the "initial configuration" or "seed". Each one of these seeds is allowed to evolve by means of the modified dynamics known as the FIRE[13] until the largest absolute value of the force, acting on every single atom, is less than a predetermined required accuracy; in our case, $10^{-9}(\varepsilon/\sigma)$. As pointed out by Bitzek et al.[13] once the required accuracy is reached, the overwhelming majority of the times it does correspond to a minimum. In fact, by minimization of 6.72×10^8 seeds for LJ_{14}, we found only one transition state (saddle point of the PES), which was reached only twice, while all the remaining hundreds of million seeds evolved toward one of the 4206 different local minima. Two configurations are defined as different if their energies differ by less than $10^{-7}\varepsilon$ or, what turns out to be equivalent for $N \leq 16$, that the parameter $D_{A,B}$ defined by

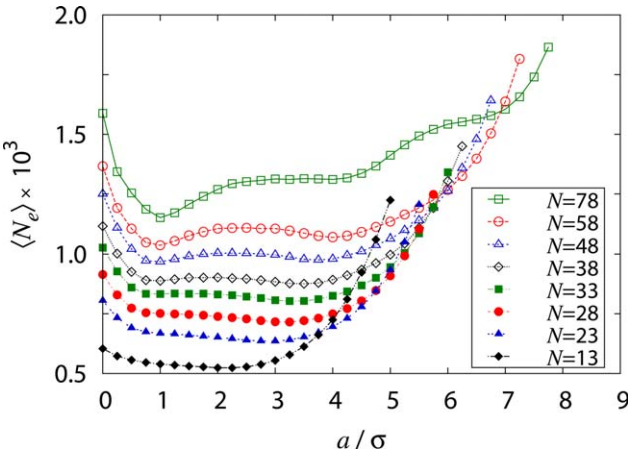

Figure 1. Average number of force evaluations $\langle N_e \rangle$ required to obtain a minimum for the Lennard–Jones pair potential, as a function of the edge length a/σ of the box used to generate the seeds, for $13 < N < 78$. For $a/\sigma=0$, we calculated with $a/\sigma=10^{-4}$.

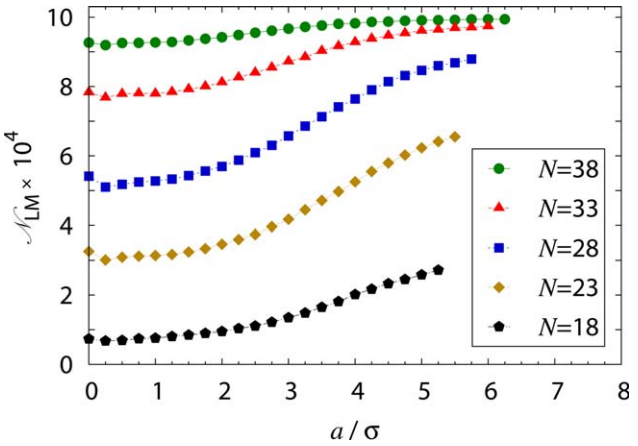

Figure 2. Diversity of configurations obtained for the LJ potential after the minimization of 10^5 seeds, as a function of the box size, for clusters of $18 \leq N \leq 38$ atoms.

eq. (1) satisfies $D_{A,B} < D_c=10^{-4}\sigma$. For $N \geq 17$, we obtained the established global minimum several times, and we checked that all of them have the same energy and structure.

Results

Seeds and the size of the initial box

Two issues that have to be tackled in an essentially unbiased search of global and local minima are: (i) the seed, or initial cluster configuration; and, (ii) the size and shape of the volume in which the dynamics are started. We choose to generate the seeds by assigning randomly spatial coordinates to the N atoms that will eventually form a cluster in a cubic box. To determine the size of the box that is most convenient for our purposes, we studied two features: (a) the number of force evaluations needed to obtain a minimum; and, (b) the diversity, understood as the number of different local minima that are generated by a certain number of seeds, for different cluster sizes (N values).

Figure 1 displays the average number of force evaluations required to minimize each one of the 10^5 seeds we investigated, as a function of the edge length a of the initial box, for different values of the number N of cluster atoms. It is noticed that for $13 \leq N \leq 65$the number of force evaluations varies smoothly as a function of the edge length. For $N < 28$, the plots show little variation in the range $1 < a/\sigma < 3$, with a shallow minimum around $2.5a/\sigma$ for $N = 13$ which becomes less profound, and shifts toward larger a/σ values, as N increases. On the other hand, a second minimum appears around $a/\sigma \sim 4$, for $N \geq 33$, and for which we have not been able to pinpoint a precise origin.

As reported by Marques et al.[31] for the LJ_{38} case, who used a big-bang method, when the volume of the box is increased the diversity that is generated increases as well, as illustrated in Figure 2. The fact that the plot for $N = 38$ is almost flat is an indication that the number of minima that we explore is tiny compared to the total number of local minima. Later on we discuss the variation of the number of minima as a function of cluster size.

Although we focus our attention on the LJ potential, our results seem to hold for other potentials as well. In particular, we tested our procedure for the Morse potential,[18,19] which by means of a single parameter ρ determines the range of the interaction, and thus adds flexibility to the model. It is given by

$$V(R)=\varepsilon \sum_{i<j} \exp\left[\rho\left(1-\frac{R_{ij}}{\sigma}\right)\right]\left\{\exp\left[\rho\left(1-\frac{R_{ij}}{\sigma}\right)\right]-2\right\}, \quad (3)$$

where R is a generic coordinate for all interatomic distances $\{R_{ij}\}$, and σ is the interatomic distance for which the pair potential reaches its minimum energy ε (i.e., the equilibrium value). The average number of force evaluations necessary to find a minimum of the Morse pair potential, as a function of the edge length of the box in which the simulations are performed, is illustrated in Figure 3.

Number of local minima

A hard problem indeed is to estimate the total number of local minima. To make some progress in that direction, we borrow from ecology the concept of rarefaction. Basically, the rarefaction curve is a plot of the number of different objects found in the process of sampling a system.[20–23] In applying it to our case, we plot the number of different local minima $\mathcal{N}_{LM}$ as a function of the number of seeds $\mathcal{N}_s$ that are explored. As is apparent in Figure 4 initially $\mathcal{N}_{LM}$ grows linearly with $\mathcal{N}_s$, but as $\mathcal{N}_s$ increases the plot flattens out and saturates. When analyzing the graph thus obtained, it is possible to determine the region one is exploring, and how well the sampling that is being used captures the existing diversity. In Figure 4, we show the rarefaction curve obtained with our method for 11-atom LJ clusters, where we distinctly observe that after 200,000 seeds are examined the number of local minima $\mathcal{N}_{LM}$ saturates.

Despite the apparent simplicity of the LJ pair potential, the precise number of local minima of the PES, even for small N

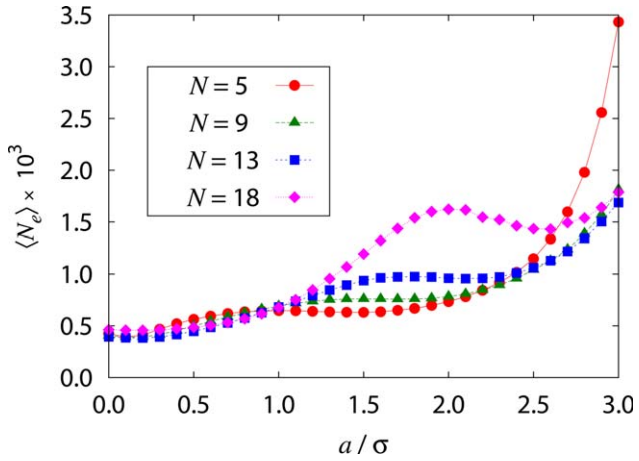

Figure 3. Average number of force evaluations $\langle N_e \rangle$ required to obtain a minimum for the Morse pair potential, as a function of the length of the edge of the box in which the initial configurations are generated. We minimized 500,000 seeds and set ρ=10. [Color figure can be viewed in the online issue, which is available at wileyonlinelibrary.com.]

values, is quite hard to estimate, and is one of the objectives we seek. An emblematic case is LJ_{13}, where the number of local minima has been continuously updated. Hoare found 988 local minima using a growth algorithm.[32,33] Later, using different variations of the eigenmode-following method,[34] Tsai and Jordan found 1328 minima.[35] Doye et al.[36] found 1467, while Ball and Berry[37] found 1478. Next, Chekmarev found 1506 minima using a taboo search of the PES.[38] Doye and Wales reported 1509 local minima,[39] and in this article we again increase this number to 1510.

For larger N values Wales and Doye,[11] citing the work of Tsai and Jordan,[35] reported the order of magnitude of the number of different local minima of the PES for LJ_{147} clusters as $\sim 10^{60}$, but with the warning that the value depends on the functional form used to fit the Tsai and Jordan results. Their estimate was obtained using the form $\exp(a+bN)$, but if one instead uses $\exp(a+bN+cN^2)$ the estimate grows to $\sim 10^{259}$

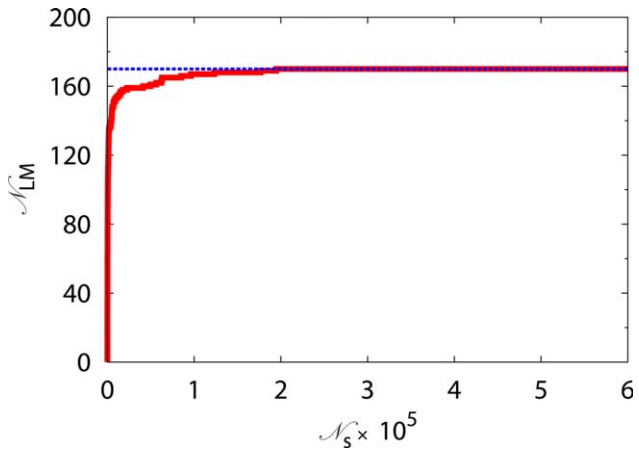

Figure 4. Rarefaction curve illustrating the evolution of the number of local minima $\mathcal{N}_{LM}$ as a function of the number of initial configurations (seeds) $\mathcal{N}_S$, for 11 atom Lennard–Jones clusters. [Color figure can be viewed in the online issue, which is available at wileyonlinelibrary.com.]

Table 1. Number of local minima estimated by various authors for LJ clusters of $N = 55$ and $N = 147$ atoms.

	$N = 55$	$N = 147$
Wales and Doye[11]	$\sim 10^{21}$	$\sim 10^{60}$ and/or $\sim 10^{259}$
Wales and Sheraga[40]	$\sim 10^{10}$	—
This work	$\sim 10^{22}$	$\sim 2\times 10^{63}$
Our results agree with the ones reported by Wales and Doye[11].		

minima. Later on, Wales and Scheraga[40] reported that the number of minima for LJ_{55}, excluding permutational isomers, is at least 10^{10}. A table with these results is given as Table 1. Considering that probably there are of the order of 10^{22} minima on the LJ_{55} PES, it is quite remarkable that it is relatively easy to obtain the global minimum, a fact underscored by Doye and Wales.[41] And finally Fournier,[42] citing Chekmarev[38] suggested that the number of local minima for an N-atom cluster, interacting through a LJ potential, is roughly of the order of $2.7^{(N-5.7)}$, for $N \geq 6$.

It is thus relevant to mention that, using the FIRE-based strategy presented here, we found all the global minima reported in the Cambridge Cluster Database[30] for the LJ pair potential up to $N = 65$. Moreover, in addition, we also found a new local minimum for LJ_{13}, which increases the number of local minima from 1509 to 1510, and 10 new local minima for LJ_{14} were also obtained, increasing their number from 4196 to 4206. For LJ_{15}, we found 11,823 local minima but, to the best of our knowledge, no estimate exists in the literature.

To check on the efficiency of our procedure, we consider the $N = 38$ case, known to be a severe test.[36] Our method finds on average the global minimum once every $\sim$7280 times, while in a recent paper Oakley et al.,[43] imposing symmetry considerations and thus slightly biasing the search, find it once every 142. Therefore, our simple and unbiased procedure seems to be quite efficient, and provides the extra bonus of generating a diverse set of low-lying local minima. However, it is worth mentioning that recently similar strategies have also been put forward in slightly different contexts by, among others, Chen et al.,[44] Lyakhov et al.,[45] and Shang et al.[46] Moreover, it is relevant to remark that there is a payoff between efficiency in obtaining the global minimum and the diversity that is generated, due to the enormous amount of local minima (our estimate is that there are $\sim 2.5\times 10^{14}$ local minima for LJ_{38}). Therefore, we understand that our procedure allows for a reasonable trade-off between efficiency and diversity.

An issue that has attracted considerable attention is how to estimate the number of minima for larger N values. On the basis of the number of local minima obtained with our strategy for $8 \leq N \leq 15$, and using the functional form $\exp(a+bN)$ to extrapolate the number of local minima to larger N values, we obtain that the number of local minima is given by $\exp(1.03368\times N - 6.12731)$, as illustrated in Figure 6, which is in close agreement with the estimate by Fournier.[42] Figure 6 also shows the number of local minima obtained after the minimization of 6×10^7 and 12×10^7 seeds, generated in a

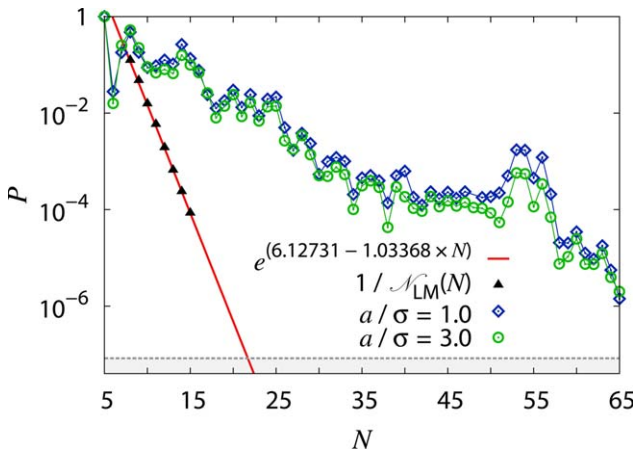

Figure 5. Probability P on a logarithmic scale (blue diamonds and green circles), of reaching the Lennard–Jones pair potential global minimum as a function of cluster size N, after minimization of 12 million seeds generated in a $1\times1\times1$ σ^3 (blue diamonds), and a $3\times3\times3$ σ^3 box (green circles). The black triangles correspond to the inverse of the number of local minima obtained, fitted by the straight red line. The shaded region at the bottom corresponds to the inverse of the number of seeds (12 million). [Color figure can be viewed in the online issue, which is available at wileyonlinelibrary.com.]

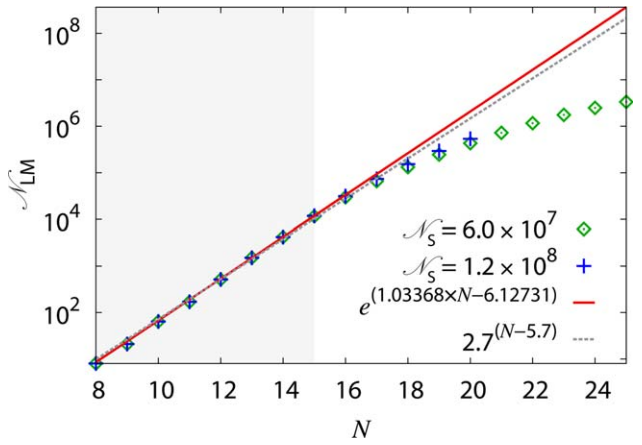

Figure 6. Number of local minima obtained for the Lennard–Jones pair potential, as a function of cluster size N, by minimization of seeds generated in a $3\times3\times3$ σ^3 box. The green diamonds and the blue + signs correspond to the 60 and 120 million seeds that were examined, respectively. The continuous red, and the dashed gray lines, correspond to two different fits, as indicated. The shaded region marks the values used for the extrapolation. [Color figure can be viewed in the online issue, which is available at wileyonlinelibrary.com.]

$3\times3\times3$ σ^3 box. It is quite apparent that there is no big difference between exploring 120 million and 60 million seeds. However, the box size strongly conditions the efficiency of the method; in fact, when using a $1\times1\times1$ σ^3 box one obtains the LJ_{38} global minimum after ~7280 minimizations, but if the box size is increased to $3\times3\times3$ σ^3 then ~23,210 minimizations are required.

The deviation of the extrapolation from our results is due to the fact that we underestimate the number of local minima, as certainly we did not find all of them. Both Fournier's and our fits roughly match the data up to $N \sim 17$. Hence, the $N = 20$ case is a good candidate to discriminate between the two curves. Furthermore, we believe that it may be possible to analyze the rarefaction curves to improve on these predictions, an issue that will be analyzed elsewhere.

Global minima

The issue of determining the ideal number of seeds that are required to explore the problem of finding the cluster global minimum, and the low-lying energy minima, is always present when one implements this type of searches. On the one hand, including a huge number of seeds lessens the probability of missing the global minimum. On the other, being overly ambitious imposes a severe stress on computing resources and machine time. Thus, exploring the field to determine convergence tendencies seems warranted. In Figure 5, we present the probability P of finding the accepted global minimum[47] by minimization of two different sets of 12 million seeds, generated in a $3\times3\times3$ σ^3 cubic box. Inspection of the figure suggests that P decreases as $\sim 10^{-N/10}$, a fact that is most important to keep in mind when trying to estimate the number of seeds required to find the energy minimum for large clusters, in the implementation of unbiased search procedures. If we define $\mathcal{N}_{LM}(N)$ as the number of local minima then, by inspection of Figure 5, we conclude that

$$P(N) > \frac{1}{\mathcal{N}_{LM}(N)} . \quad (4)$$

In fact, for all the cluster sizes, we explored (i.e., $N \leq 65$), our procedure always yields the accepted global minimum.

Up to now, the only unbiased methods which are able to obtain the global minimum for the LJ Marks decahedra for N=75−77 and N=102−104 are BH and the GA. At this point, we have minimized 12,000,000 seeds for the $N = 75$ case, without obtaining the reported global minimum.

Lowest energy planar clusters

It is well-known that, regardless of the element, the lowest energy cluster configuration obtained with phenomenological potentials is not necessarily the same as the lowest energy structures of DFT calculations.[9,48–51] Because of this reason, a widely used strategy to obtain the global minimum of a given configuration is to minimize, using DFT, a large set of low-energy configurations obtained by means of phenomenological potentials. However, even when one is able to determine all the local minima of a phenomenological potential it is possible that none of them matches, or converges toward, the global minimum after DFT refinement. A clear-cut example is found in the few atom transition and coinage metal clusters ($N \sim 10$), where it is often the case that the global minimum is a planar configuration.[49] And, as it is well-known that LJ, Morse, and the widely used for transition metals Gupta potential, they do not yield planar structures among the set of local minima. On the contrary, our method has the rather unique capability of creating planar seeds which remain planar throughout the FIRE minimization. This is a useful feature which allows to generate low-energy planar configurations. Of

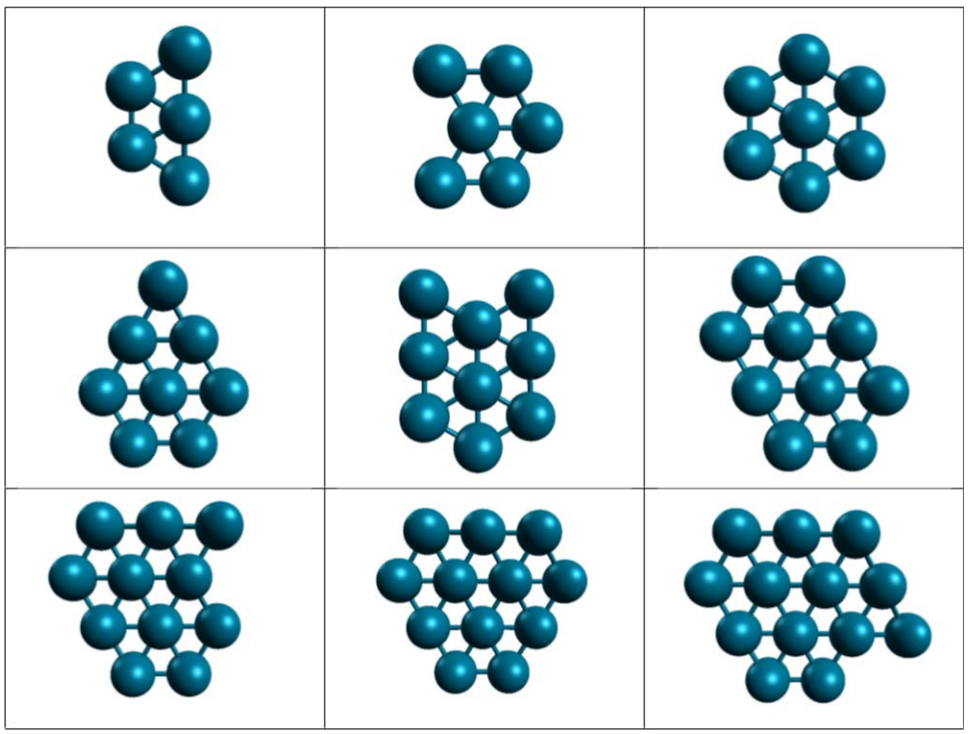

Figure 7. Conformations of the lowest energy planar LJ configurations, for clusters of $5 \leq N \leq 13$ atoms. [Color figure can be viewed in the online issue, which is available at wileyonlinelibrary.com.]

course, these structures are not stable local minima of the arbitrary phenomenological potential used, but they provide a valuable contribution to the overall structure diversity, which is a valuable tool in the search for two-dimensional (2D) minima. In Table 2, we provide the number of planar local energy minima and their energies E in units of ε, for clusters of up to 13 atoms, obtained after minimization of 60 million seeds. In Figure 7, we illustrate the lowest energy configurations we obtained for LJ clusters of $5 \leq N \leq 13$ atoms. These conformations are by no means stable minima of the 3D phenomenological potential that is used, but they serve the purpose of convenient inputs for DFT refinement, especially suited when a 2D quantum global minimum can be expected.[51,52] This is due to the fact that with this procedure planar seeds remain planar throughout.

Table 2. Number of local energy minima obtained for planar configurations, and the corresponding values of the minimal energies.

No. of atoms	No. of configurations	E/ε
3	1	−3.000000
4	1	−5.073421
5	1	−7.178024
6	3	−9.358274
7	4	−12.534867
8	9	−14.683990
9	16	−16.909315
10	36	−20.101612
11	70	−22.336540
12	160	−25.566703
13	337	−27.804065

Minima distribution and basin sizes

Interesting information is contained in the mean square distance deviation $\langle\sigma\rangle$, as a function of the average interatomic distances $\langle d_{ij}\rangle$, of the local minima defined as

$$\langle\sigma\rangle = \sqrt{\frac{2}{N(N-1)}\sum_{i\neq j}^{N}\left(r_{ij}-\langle d_{ij}\rangle\right)^2}\,, \tag{5}$$

and

$$\langle d_{ij}\rangle = \frac{2}{N(N-1)}\sum_{i\neq j}^{N} r_{ij}\,. \tag{6}$$

For the $N = 9$ cluster, we obtain the spectrum of the 21 minima that is displayed in the top panel of Figure 8. A prominent feature is the clear-cut energy gap between the global minimum and the other 20 local minima. This feature is present in all of the spectra we have calculated, that is up to $N \leq 14$, as can be verified in Figure 9. If proved to be general, it would constitute a useful tool in the problem of searching for the global minimum. The structure of the new local minimum for $N = 13$ is illustrated in Figure 10. Another general property that Figures 8 and 9 display is that the global minimum always corresponds to lowest value of $\langle d_{ij}\rangle$ and to low values of $\langle\sigma\rangle$, a fact that is most salient for the symmetric (icosahedral) $N = 13$ case where the global minimum splits off completely, and corresponds to the smallest of all $\langle d_{ij}\rangle$ and $\langle\sigma\rangle$ values.

A second characteristic that is noticeable in Figures 8 and 9 is that in general P reaches a rather large value for the global

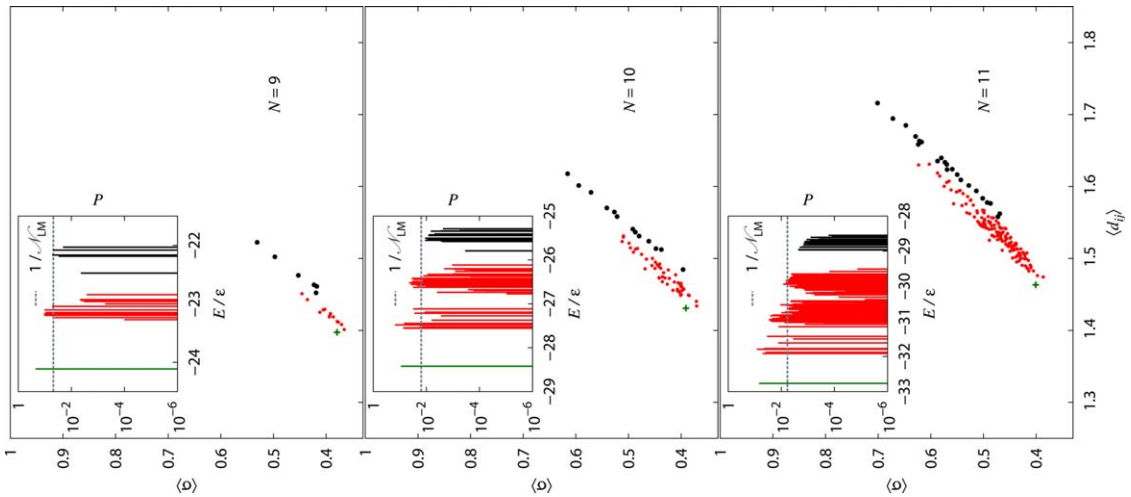

Figure 8. Mean square deviation $\langle\sigma\rangle$ versus mean interatomic distance $\langle d_{ij}\rangle$ for $N = 9$, 10, and 11 atom LJ clusters. The inset, color coded as in the main figure, corresponds to the spectrum of the probability for finding local minima as a function of energy. The dark green bars and + signs correspond to the global minima. [Color figure can be viewed in the online issue, which is available at wileyonlinelibrary.com.]

minimum, which implies that it is hit several times in the search process. Moreover, when one looks at the energy values of the previously unreported local minima we found for $N = 13$, and illustrated in Figure 10, and the 10 new minima for $N = 14$, these are located in the midst of the distribution, rather than at the largest energy values, as one naively could have expected. Thus, that they were previously missed seems to be related to their narrow basin of attraction widths. The only transition state (saddle point of the PES) that we found, as already aforementioned, (marked with an arrow in Fig. 9), has an energy of $E/\varepsilon \approx -46$.

Inspection of Figure 9 also suggests that for large clusters ($N \gg 1$) the probability spectrum does have a well-separated global minimum and that P displays a rather strong decrease as a function of increasing energy (notice the logarithmic character of the plots). In addition, the breaking up of the spectrum into "energy bands" seems to be a general attribute of small clusters. Moreover, Figures 8 and 9 display another interesting feature, namely that the structures in a particular energy band also appear as segregated layers in the $\langle\sigma\rangle$ versus $\langle d_{ij}\rangle$ plot, a fact we stress with the different color codes used in these figures.

We stress that the size of the global minimum attraction basin is among the largest ones, as can be observed by inspection of Figures 8 and 9. The rest of the basin sizes is, on average, a monotonously decreasing function of energy.

Discussion and Conclusions

A strategy to find a large set of diverse cluster energy minima is developed. Although at present we restrict ourselves to interactions specified by classical potentials, the procedure can

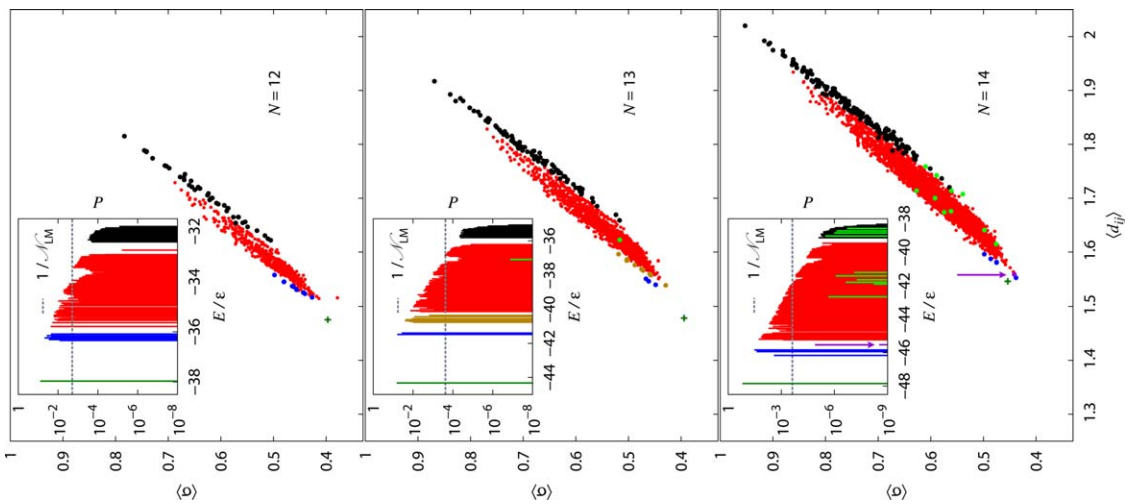

Figure 9. Mean square deviation $\langle\sigma\rangle$ versus mean interatomic distance $\langle d_{ij}\rangle$ for $N = 12$, 13, and 14 atom LJ clusters. The bright green bars and dots label the new minima we found. The inset, color coded as in the main figure, corresponds to the spectrum of the probability for finding local minima as a function of energy. The arrows in the $N = 14$ figure denote the transition point. The dark green bars and + signs correspond to the global minima. [Color figure can be viewed in the online issue, which is available at wileyonlinelibrary.com.]

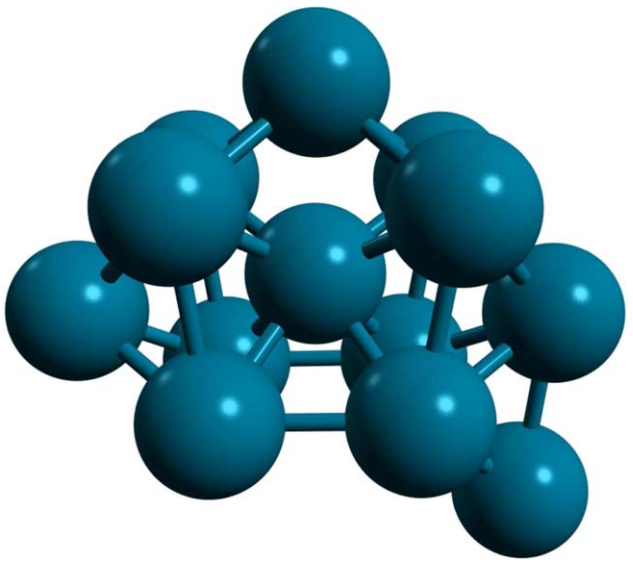

Figure 10. Conformation of the new local minimum for LJ_{13}, with an energy $-37.090027\,E/\varepsilon$ and C_S symmetry. [Color figure can be viewed in the online issue, which is available at wileyonlinelibrary.com.]

be implemented as well in combination with *ab initio* calculations. It is inspired on the premise that diversity is the key ingredient to obtain, via *ab initio* refinement, the putative global minimum for a small cluster. Thus, our primary objective is to develop a procedure to obtain a significant majority of the local minima of a PES. The strategy we implemented is based on the FIRE algorithm, which combines molecular dynamics with velocity modifications and adaptive time steps. Our strategy succeeds in finding all the reported global minima for clusters of up to 65 atoms, interacting via a LJ potential. Moreover, one new local minimum is found for LJ_{13} and 10 new ones for LJ_{14}. Although we devoted most of our interest to the LJ potential, the method seems to be applicable to other pair potentials, like the one due to Morse.

An issue we studied in detail is the influence of the size of the initial box for clusters of up to 78 atoms, in terms of the average number of force evaluations required to obtain a minimum for the LJ potential. Another subject we investigated is how to estimate the number of local minima of the PES, which grows explosively with cluster size. Based on the exploration of up to 120 million seeds, we are able to conjecture an extrapolation based on the number of different local minima for LJ_N, with $8 \leq N \leq 15$. In addition, the consequences of the choice of an appropriate box size on the diversity of the minima obtained, and the two minima of Figures. 1 and 3 seem to be features that apply to other potentials, besides LJ. In addition, we provide an estimate of the number of seeds that are required to find the global minimum. The FIRE algorithm has the additional advantage that it allows to introduce planar low energy configurations in the diverse set, as they remain planar during the FIRE minimization process. This feature is most relevant when searching for the DFT minima of coinage metal clusters of up to 20 atoms, as *ab initio* calculations have shown that the putative global minima is planar, and phenomenological potentials do not yield planar minimum energy conformations.

The energy distribution of the local minima is investigated using a tool introduced by ecologists: the rarefaction curve, which is a plot of the number of different objects that is found in the process of sampling a system. The saturation of the rarefaction plot allows an educated guess on how many seeds are to be explored to obtain the putative global minimum and most of the local minima.

The plot of the probability P of finding a local minimum, as a function of energy, provides additional information. We observe that P breaks up into energy bands, and that the ground state splits off. Moreover, P exhibits a rapid decrease as a function of energy. In addition, it is remarkable that the lowest energy configurations we investigated corresponds to a minimum of the mean square deviation $\langle\sigma\rangle$ versus mean interatomic distance $\langle d_{ij}\rangle$. It is our intention to explore this feature in more detail and to use it to improve the code convergence. Moreover, the procedure we put forward compares quite favorably with the methods found in the literature like BH, Minima Hopping,[12] and Symmetrization Core Orbital.[43]

In summary, we implemented an efficient strategy to find energy minima of cluster conformations, when the atoms interact via phenomenological potentials. The objectives of obtaining the global minimum as well as a diverse set of low-lying local minima by means of a rather simple procedure were reached, as our strategy recovers all the reported minima, finds a fair number of new ones, and generates a large diversity of configurations, including planar ones, which are functional as inputs for *ab initio* refinement.

Keywords: optimization · global minimum · local minima · Lennard–Jones pair potential · energy landscape

How to cite this article: J. Rogan, A. Varas, J. A. Valdivia, M. Kiwi. *J. Comput. Chem.* **2013**, *34*, 2548–2556. DOI: 10.1002/jcc.23419

[1] S. Goedecker, W. Hellmann, T. Lenosky, *Phys. Rev. Lett.* **2005**, *95*, 055501.
[2] Z. Li, H. A. Scheraga, *Proc. Natl. Acad. Sci.* **1987**, *84*, 6611, ISSN 0027-8424.
[3] J. Rogan, R. Ramírez, A. H. Romero, M. Kiwi, *Eur. Phys. J. D* **2004**, *28*, 219, ISSN 1434-6060.
[4] R. H. Leary, *J. Global Optim.* **1997**, *11*, 35.
[5] F. Aguilera-Granja, A. Vega, J. Rogan, X. Andrade, G. García, *Phys. Rev. B* **2006**, *74*, 224405, ISSN 1098-0121.
[6] J. Rogan, G. García, M. Ramírez, V. Muñoz, J. A. Valdivia, X. Andrade, R. Ramírez, M. Kiwi, *Nanotechnology* **2008**, *19*, 205701, ISSN 0957-4484.
[7] B. Hartke, *Chem. Phys. Lett.* **1996**, *258*, 144.
[8] J. Lee, I. -H. Lee, J. Lee, *Phys. Rev. Lett.* **2003**, *91*, 1, ISSN 0031-9007.
[9] J. Rogan, G. García, C. Loyola, W. Orellana, R. Ramírez, M. Kiwi, *J. Chem. Phys.* **2006**, *125*, 214708.
[10] J. Rogan, M. Ramírez, V. Muñoz, J. A. Valdivia, G. García, R. Ramírez, M. Kiwi, *J. Phys. Condensed Matter* **2009**, *21*, 084209, ISSN 0953-8984.
[11] D. J. Wales, J. P. K. Doye, *J. Phys. Chem. A* **1997**, *101*, 5111, ISSN 1089-5639, available at: http://pubs.acs.org/doi/abs/10.1021/jp970984n.
[12] S. Goedecker, *J. Chem. Phys.* **2004**, *120*, 9911.

[13] E. Bitzek, P. Koskinen, F. Gähler, M. Moseler, P. Gumbsch, *Phys. Rev. Lett.* **2006**, *97*, 170201, ISSN 0031-9007.
[14] E. Machado-Charry, L. K. Béland, D. Caliste, L. Genovese, T. Deutsch, N. Mousseau, P. Pochet, *J. Chem. Phys.* **2011**, *135*, 034102.
[15] J. A. Flores-Livas, M. Amsler, T. J. Lenosky, L. Lehtovaara, S. Botti, M. A. L. Marques, S. Goedecker, *Phys. Rev. Lett.* **2012**, *108*, 117004.
[16] M. Amsler, J. A. Flores-Livas, L. Lehtovaara, F. Balima, S. A. Ghasemi, D. Machon, S. Pailhès, A. Willand, D. Caliste, S. Botti, A. San Miguel, S. Goedecker, M. A. L. Marques, *Phys. Rev. Lett.* **2012**, *108*, 065501.
[17] A. Ishii, H. Kimizuka, S. Ogata, *Comput. Mat. Sci.* **2012**, *54*, 240.
[18] P. M. Morse, *Phys. Rev.* **1929**, *34*, 57.
[19] J. M. Marques, A. A. Pais, P. E. Abreu, *J. Comput. Chem.* **2012**, *33*, 442, ISSN 1096-987X.
[20] H. L. Sanders, *Am. Nat.* **1968**, *102*, 243.
[21] K. I. Ugland, J. S. Gray, K. E. Ellingsen, *J. Anim. Ecol.* **2007**, *72*, 888.
[22] A. Chiarucci, G. Bacaro, D. Rocchini, L. Fattorini, *Community Ecol.* **2008**, *9*, 121.
[23] J. Orlando, M. Carú, B. Pommerenke, G. Braker, *Front. Microbiol.* **2012**, *3*, 101.
[24] J. Nocedal, *Math. Comp.* **1980**, *35*, 773.
[25] V. G. Grigoryan, M. Springborg, *Chem. Phys. Lett.* **2003**, *375*, 219, ISSN 00092614.
[26] A. R. Oganov, M. Valle, *J. Chem. Phys.* **2009**, *130*, 104504.
[27] J. M. Dieterich, H. Bernd, *J. Comput. Chem.* **2011**, *32*, 1377.
[28] X. Lai, W. Huang, R. Xu, *J. Phys. Chem. A* **2011**, *115*, 5021, ISSN 1520-5215.
[29] X. Lai, R. Xu, W. Huang, *Sci. China Chem.* **2011**, *54*, 985, ISSN 1674-7291.
[30] D. J. Wales, J. P. K. Doye, A. Dullweber, M. P. Hodges, F. Y. Naumkin, F. Calvo, J. Hernández-Rojas, T. F. Middleton, *The Cambridge Cluster Database*, available at: http://www-wales.ch.cam.ac.uk/CCD.html.
[31] J. M. C. Marques, A. A. C. C. Pais, P. E. Abreu, *J. Comput. Chem.* **2010**, *31*, 1495.
[32] R. M. Hoare, *Adv. Chem. Phys.* **1979**, *40*, 49.
[33] R. M. Hoare, J. A. McInnes, *Adv. Phys.* **1979**, *32*, 791.
[34] C. J. Cerjan, W. H. Miller, *J. Chem. Phys.* **1981**, *75*, 2800.
[35] C. J. Tsai, K. D. Jordan, *J. Phys. Chem.* **1993**, *97*, 11227, ISSN 0022-3654.
[36] J. P. K. Doye, M. A. Miller, D. J. Wales, *J. Chem. Phys.* **1999**, *111*, 8417.
[37] K. D. Ball, R. S. Berry, *J. Chem. Phys.* **1999**, *111*, 2060.
[38] S. Chekmarev, *Phys. Rev. E* **2001**, *64*, 1, ISSN 1063-651X.
[39] J. P. K. Doye, D. J. Wales, *J. Chem. Phys.* **2002**, *116*, 3777, ISSN 00219606.
[40] D. J. Wales, H. A. Scheraga, *Science* **1999**, *285*, 1368, ISSN 00368075.
[41] J. P. K. Doye, D. J. Wales, *Z. Phys. D.* **1997**, *40*, 194.
[42] R. Fournier, *J. Chem. Theor. Comput.* **2007**, *3*, 921, ISSN 1549-9618.
[43] M. T. Oakley, R. L. Johnston, D. J. Wales, *Phys. Chem. Chem. Phys.* **2013**, *15*, 3965, available at: http://dx.doi.org/10.1039/C3CP44332A.
[44] Z. Chen, X. Jiang, J. Li, S. Li, L. Wang, *J. Comput. Chem.* **2013**, *34*, 1046.
[45] A. O. Lyakhov, A. R. Oganov, H. T. Stokes, Q. Zhu, *Comput. Phys. Comm.* **2013**, *184*, 1172.
[46] C. Shang, Z. -P. Liu, *J. Chem. Theory Comput.* **2013**, *9*, 1838.
[47] D. J. Wales, J. P. K. Doye, *J. Phys. Chem. A* **1997**, *101*, 5111.
[48] C. M. Chang, M. Y. Chou, *Phys. Rev. Lett.* **2004**, *93*, 133401.
[49] F. Muñoz, J. Rogan, G. García, M. Ramírez, J. A. Valdivia, R. Ramírez, M. Kiwi, *Eur. Phys. J. D* **2011**, *61*, 87.
[50] F. Muñoz, J. Rogan, G. García, J. A. Valdivia, R. Ramírez, M. Kiwi, *Eur. Phys. J. D* **2011**, *64*, 45.
[51] F. Muñoz, J. Rogan, J. A. Valdivia, A. Varas, M. Kiwi, *Physica B* **2013**, *427*, 76.
[52] F. Häkkinen, *Chem. Soc. Rev.* **2008**, *37*, 1847.

Received: 5 March 2013
Revised: 25 July 2013
Accepted: 4 August 2013
Published online on 26 August 2013